Polymer 50 (2009) 598–604

Contents lists available at ScienceDirect

Polymer

journal homepage: www.elsevier.com/locate/polymer

Biaxially oriented poly(propylene-*g*-maleic anhydride)/phosphate glass composite films for high gas barrier applications

Mohit Gupta, Yijian Lin, Taneisha Deans, Alexis Crosby, Eric Baer, Anne Hiltner, David A. Schiraldi*

Department of Macromolecular Science and Engineering, NSF Center for Layered Polymeric Systems, Case Western Reserve University, 2100 Adelbert Road, Cleveland, OH 44106, USA

ARTICLE INFO

Article history:
Received 25 August 2008
Received in revised form
13 November 2008
Accepted 15 November 2008
Available online 24 November 2008

Keywords:
Phosphate glass
Polypropylene
Orientation

ABSTRACT

The solid state structure and oxygen transport properties of biaxially oriented poly(propylene-*graft*-maleic anhydride) (PPgMA) reinforced with a low glass transition temperature (T_g) phosphate glass (Pglass) were investigated. Composites were prepared by melt blending PPgMA with up to 20 volume% Pglass. Melt blended composites were compression molded into monolayer structures and then biaxially stretched at a temperature above the T_g of the Pglass. Scanning electron microscopy confirmed that biaxial stretching transformed the spherical Pglass particles into platelets oriented in the plane of the film. Gas transport measurements revealed a reduction in the oxygen permeability by as much as 2 orders of magnitude compared to the unoriented PPgMA film. The permeability was analyzed according to performance models for dispersions of platelet-like fillers proposed by Cussler and Nielson. Aspect ratios ranging from 15 to 80 were obtained by fitting the experimental data to the models. Mechanical tests revealed that blending with Pglass increased the modulus of the stretched film but reduced the elongation at break only slightly.

1. Introduction

Incorporation of solid inorganic fillers with high aspect ratios has been widely examined as an approach to improve gas barrier properties of polymers. Alignment of overlapping platelet particles can greatly increase the diffusion distance and barrier properties by creating a tortuous path for the diffusing species [1,2]. Incorporating such fillers in large amounts complicates processing due to the inherent increases in melt viscosity. Phosphate glasses possessing low glass transition temperatures (T_g) which display both water resistance and chemical durability have been described in the literature [3–7]. These phosphate glasses are fluidic over a range of temperatures that includes the melt processing temperature of many different polymers. It is therefore possible to process these inorganic glasses with organic polymeric materials using conventional processing methodologies to yield composite materials containing phosphate glass loadings as high as 60–90 wt% [8–10].

There is considerable interest in the development of polymers with high barrier to oxygen, carbon dioxide, water, or organic vapors for use in the packaging industry. Biaxially oriented polypropylene (BOPP) film has been widely used for food packaging but does exhibit sufficiently high oxygen barrier properties for some applications [11]. The present work aims to utilize low T_g inorganic glasses as impermeable inclusions in polypropylene. The choice of glasses is predicated on their plastic deformation from small droplets into high aspect ratio platelets during the biaxial stretching process. The platelet morphology would not only improve the barrier properties but would also lead to significant improvement in mechanical properties thus opening up new application areas for these materials. In this study, poly(propylene-*graft*-maleic anhydride) (PPgMA) was melt blended with a low glass transition temperature phosphate glass and then biaxially stretched in order to obtain high aspect ratio platelets. The morphology and oxygen permeability of PPgMA/Pglass composite films were evaluated as a function of glass content and draw ratio.

2. Experimental

2.1. Materials

The poly(propylene-*graft*-maleic anhydride) PPgMA grade PB 3002 was provided by Chemtura Corp. The density and melt flow index (MFI) were 0.91 g cm^{-3} and 7 g (10 min)$^{-1}$ (ASTM D 1238), respectively. The polypropylene (PP) grade ZN5D98 was provided by The Dow Chemical Company. The density and melt flow index (MFI) were 0.9 g cm^{-3} and 3.4 g (10 min)$^{-1}$ (ASTM D 1238), respectively. Glasses were prepared from reagent grade tin fluoride (SnF_2), tin oxide (SnO) and ammonium dihydrogen phosphate ($NH_4H_2PO_4$) all purchased from Aldrich and used as received.

* Corresponding author. Tel.: +1 216 368 4243; fax: +1 216 368 4202.
E-mail address: david.schiraldi@case.edu (D.A. Schiraldi).

0032-3861/$ – see front matter © 2008 Elsevier Ltd. All rights reserved.
doi:10.1016/j.polymer.2008.11.018

Table 1
Batch glass compositions in mol% and properties (batch size approx. 25 g).

	Pglass 1	Pglass 2	Pglass 3	Pglass 4	Pglass 5
P_2O_5	30	35	40	30	30
SnO	20	15	10	15	10
SnF_2	50	50	50	55	60
Density (g/cm^3)	3.65 ± 0.01	3.30 ± 0.01	3.12 ± 0.01	3.62 ± 0.01	3.60 ± 0.01
Measured T_g (°C)	118 ± 2	110 ± 2	98 ± 2	112 ± 2	105 ± 2
Synthesis temp. (°C)	450	450	450	450	450
Synthesis time (min)	15	15	15	15	15
Observation	Clear glass	Clear glass	Clear glass	Clear glass	Clear glass

2.2. Glass preparation

The phosphate glasses (Pglass) were prepared on a 250 g scale. The ingredients were carefully weighed and added into a closed jar to form Pglass with a batch molar composition of 50% $SnF_2 + 20\%$ $SnO + 30\%$ P_2O_5. The ingredients were tumble mixed for 25–30 min to produce a uniform mixture and then transferred to a 300 ml capacity vitreous carbon crucible. The crucible was placed, uncovered, into a muffle furnace at 450 °C for 70 min. Fluid melts obtained using this procedure were quenched onto a stainless steel plate and annealed by placing in the oven at approximately 20 °C above the T_g for about 90 min [4,7]. This results in a Pglass with a density of 3.65 ± 0.01 g cm^{-3} and a T_g of 118 ± 2 °C.

2.3. Composite preparation

The composites containing 6, 10 and 20 volume% Pglass were prepared using a Thermo-Haake Rheomix 600 batch mixer equipped with roller rotors. The polymer and Pglass were batch mixed at 210 °C at a rotor speed of 60 rpm for 8 min, then collected as pieces about 2 mm thick and 100 mm × 100 mm across. The polymer was dried in a vacuum oven at 100 °C for at least 24 h prior to melt blending. The Pglass used was fine powder ground using an IKA M20 mill and stored in a desiccator before use in order to prevent any moisture absorption. Ground Pglass, when exposed to atmosphere for a couple of days under normal laboratory temperature and humidity absorbs moisture reversibly. The T_g drops as much as 10–20 °C, however, drying the glass under vacuum at temperature above its T_g brings the T_g to its original value.

2.4. Film preparation

Films approximately 0.25 mm thick were prepared by compression molding the composite material between two steel plates covered with Kapton® polyimide films in a Carver press at 210 °C, 5 min residence time at 5000 psi pressure. The films were quenched by placing between two cold platens after removal from the press. The films were stored in a desiccator to prevent any water absorption.

2.5. Biaxial orientation

Square specimens 85 mm × 85 mm were cut from the compression-molded sheets, marked with a grid pattern, and biaxially stretched in a Brückner Karo IV biaxial stretcher at 155 °C at engineering strain rates of 400% s^{-1} and 5% s^{-1} based on the original specimen dimensions. The preheat time before stretching was fixed at 1 min. The sheets were simultaneously and equi-biaxially drawn to draw ratios varying from 3×3 to 5×5. The uniformity of the drawn specimens was determined from the even deformation of the grid pattern.

2.6. Morphological analysis

In order to analyze the morphology of the composite materials before and after biaxial orientation, the films were embedded in epoxy and microtomed at room temperature using a glass knife. The samples were sputter coated with palladium. The morphology was observed using a Philips XL scanning electron microscope (SEM).

2.7. Image analysis

SEM images were analyzed using Image-Pro Plus software in order to estimate the average diameter of the dispersed Pglass droplet. Three different images were analyzed for each composition and the values were averaged to obtain the reported results.

2.8. Oxygen permeability

Oxygen flux $J(t)$ at 0% relative humidity, 1 atm and 23 °C was measured with a MOCON OX-TRAN 2/20. The permanent gas stream was diluted with nitrogen to achieve a 2% oxygen concentration in order to avoid exceeding the detector capability of the instrument. Permeability was obtained from the steady flux J_o according to

$$P = J_o l / p \tag{1}$$

where p is the oxygen pressure and l is the film thickness. Two films prepared under the same conditions were tested to obtain the average permeability. The permeability can be split into the solubility (S) and diffusivity (D). Usually D and S are extracted from the

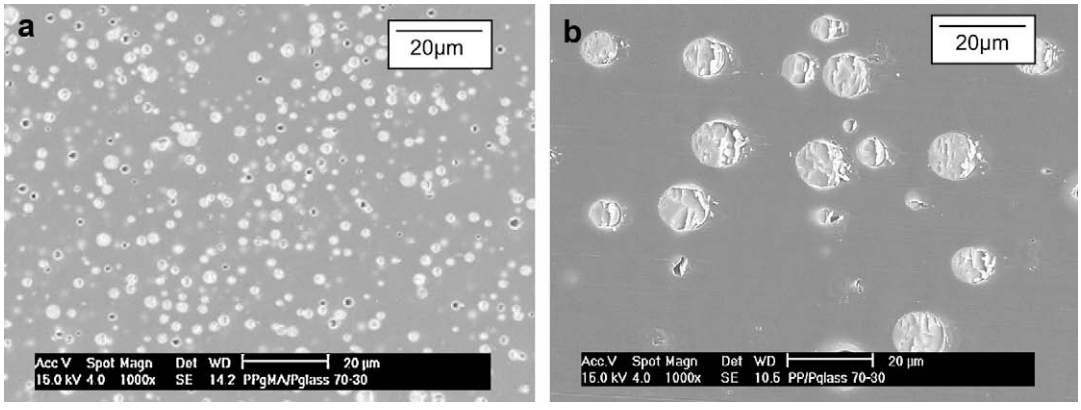

Fig. 1. SEM images of compression molded 90/10 v/v composites (a) PPgMA/Pglass (b) PP/Pglass.

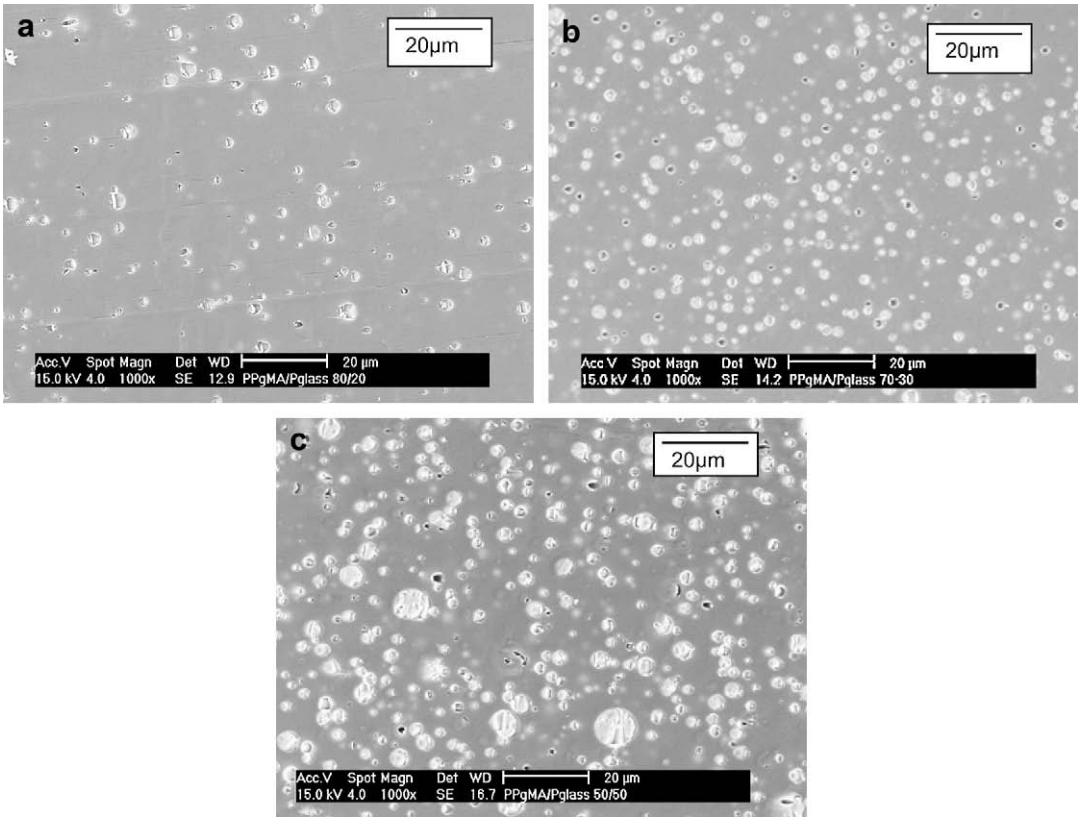

Fig. 2. SEM images of compression molded PPgMA/Pglass composites (a) 94/6 v/v (b) 90/10 v/v (c) 80/20 v/v.

non-steady state flux curve. This is difficult if the films are thin. In this study the films after biaxial orientation were 5–8 μm thick and the steady state was achieved very rapidly. It was not possible to extract *D* and *S* even for the higher barrier films.

2.9. Density measurements

The density was measured at room temperature according to ASTM D1505-85. A 2-propanol/water gradient column with a range of 0.85–0.95 g cm^{-3} and two different calcium nitrate/water columns having a range of 1.05–1.20 g cm^{-3} and 1.30–1.46 g cm^{-3} were prepared and calibrated with glass floats of known density. Small pieces of film ($\sim 5 \times 5$ mm^2) were placed in the column and measurements were taken after 10–12 h equilibration. At least 3 pieces from each film were tested.

Densities of the prepared glasses were measured using Archimedes method with deionized water as the immersion fluid.

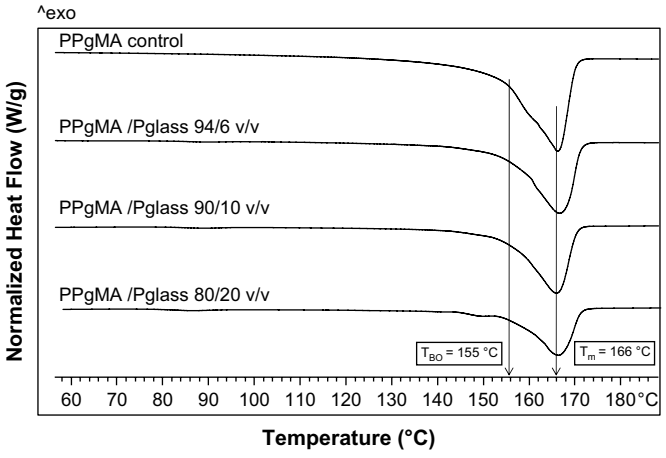

Fig. 3. First heating thermograms of PPgMA/Pglass composites.

2.10. Mechanical properties

Mechanical properties of the composite materials were evaluated in uniaxial tension on an Instron 5565 universal tester. Film samples were punched into dog bone shape using an ASTM-D638V punch tool and tested at room temperature at a strain rate of 10%/min. Three samples were tested for each composition and the values were averaged to obtain the reported results.

3. Results and discussion

Phosphate glasses containing 10–20 mol% SnO were prepared in 25 g batches using vitreous carbon crucible by melting for 15 min at 450 °C. The batch compositions for these materials are listed in Table 1 along with their appearances.

Previous studies on Pglasses based on a ternary system of SnO–SnF_2–P_2O_5 had shown that the properties of these glasses are

Table 2
Comparison of the draw ratio at different strain rates for neat PPgMA films biaxially oriented at 155 °C.

Strain rate (s^{-1})	Targeted draw ratio	Measured draw ratio (approx.)	A/A_o
400	3 × 3	3.8 × 3.8	14.5
400	4 × 4	5.0 × 5.0	25.0
400	5 × 5	5.6 × 6.0	33.6
5	3 × 3	5.5 × 6.0	33.0
5	4 × 4	7.2 × 8.0	57.6
5	5 × 5	8.5 × 8.5	70.0

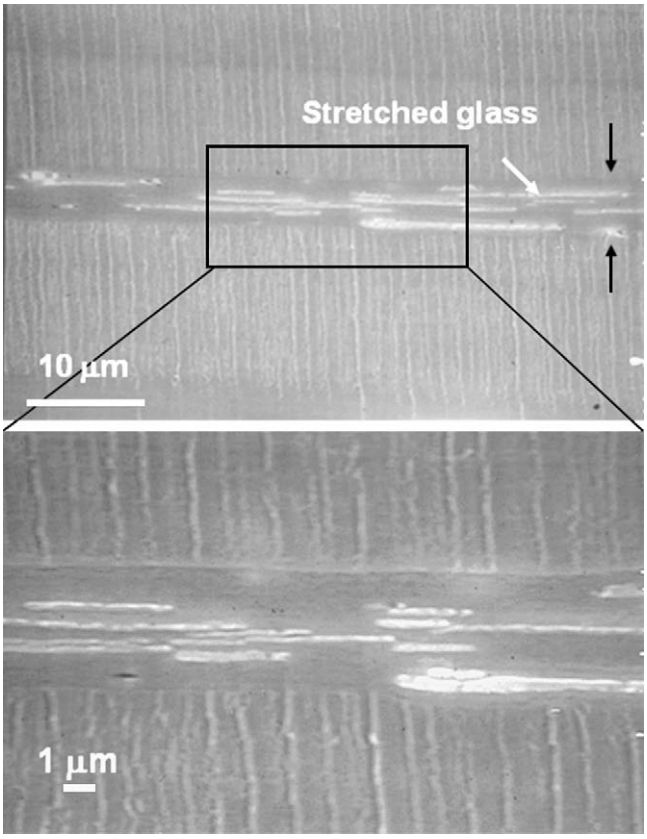

Fig. 4. SEM images of biaxially oriented PPgMA/Pglass 90/10 v/v composite; targeted draw ratio (λ) = 4 × 4.

extremely sensitive to variations in melting history such as the synthesis time and temperature [3–7]. Differences in T_g have been observed for what was supposed to be the same glass compositions prepared by different authors and can be attributed to small differences in preparation methods (it should be noted that removal of volatile reaction products drives the glass formation reaction, and can be subject to reactor surface area:volume ratio, for example) [7,9]. Addition of SnO to SnF_2–P_2O_5 has been in general found to decrease the volatility of the melt and increase the chemical durability of the glass [5]. Pglass produced with a batch molar composition of 50% SnF_2 + 20% SnO + 30% P_2O_5 has been shown to have sufficiently high chemical durability and has been successfully melt blended with a variety of different organic polymers [4,7,10]. Similar observations were made in our limited study with these glasses. Hence, for our study this particular composition was chosen for scaling up the synthesis and the synthesis procedure is given in experimental section.

Composites were prepared by melt mixing ground Pglass with two different organic thermoplastic polymers, PP and PPgMA. The properties of polymer blends are usually controlled by the properties of the components, the morphology of the blends, and the interaction between components in the blends [12–16]. The domain size is often used to indicate the extent of compatibility of multiphase polymer systems, i.e., the smaller the domain size, the more compatible the systems are and the better the mechanical properties [14–16]. Fig. 1 shows the microstructure for PP/Pglass and PPgMA/Pglass 90/10 v/v composites. The SEM images clearly demonstrate that the size of the dispersed Pglass droplets was much smaller in PPgMA/Pglass composites suggesting better interfacial adhesion between the Pglass and the polymer matrix. The hydrogen bonding between the hydroxyl groups on the glass surface and the maleic anhydride group in PPgMA is believed to be the reason for improved interfacial adhesion. The discussion which follows will be limited to composites of PPgMA and Pglass.

The typical morphologies of PPgMA/Pglass 94/6, 90/10 and 80/20 v/v composites obtained by melt mixing are shown in Fig. 2. The Pglass was dispersed as spherical droplets in the polymer matrix after melt mixing. The SEM images were analyzed using image analysis software in order to estimate the average diameter of the dispersed droplet phase in the composites. The average particle size increased slightly with increasing volume% Pglass from 2.1 ± 1.0, to 2.2 ± 0.8 to 2.5 ± 1.3 μm for the 94/6, 90/10 and 80/20 v/v composites, respectively.

4. Biaxial orientation

Thermograms of the compression molded PPgMA and PPgMA/Pglass films showed a gradual onset of melting at about 140 °C and the peak melting temperature at 166 °C, Fig. 3. At 155 °C, the temperature used to perform the stretching, the films were partially melted. Stretching at lower temperatures resulted in void formation in the case of composite films. With increasing temperature, the stress response decreased as more crystals melted [17]. An optimum balance in stress response and orientation was achieved for the composites at 155 °C. The film was preheated at 155 °C for 60 s and stretched at a strain rate of 400% s^{-1} or 5% s^{-1}. A grid pattern was marked on the sheet before stretching in order to determine the uniformity of the deformation and to obtain an accurate measure of the draw ratio. The draw ratio in the two orthogonal directions was calculated from the change in separation of the parallel grid lines. The area draw ratio A/A_o was also obtained, where A_o is the initial area defined by the grid lines and A is the area defined by the same grid lines after stretching.

For the films stretched at 400% s^{-1}, the biaxial draw ratio in the center region of the stretched film was very uniform as indicated by straight, parallel grid lines, and was close to the target draw ratio, Table 2. However, examination of the films revealed that the glass particles debonded from the matrix and were not deformed during the stretching process. In the case of films stretched at 5% s^{-1}, the measured draw ratio in the center region of the film was substantially higher than the target draw ratio, Table 2. It was thought that uniformity was affected by uneven heating. Especially with an unusually low stretch rate, a slightly higher temperature in the center of the stretching chamber could result in uneven drawing.

Table 3
Oxygen permeability of biaxially oriented PPgMA and PPgMA/Pglass composites for target draw ratios of 1 × 1, 3 × 3, 4 × 4 and 5 × 5.

Sample	P (O_2) (barrer)				Improvement in barrier			
	1 × 1	3 × 3	4 × 4	5 × 5	1 × 1	3 × 3	4 × 4	5 × 5
PPgMA	0.90 ± 0.04	0.65 ± 0.03	0.57 ± 0.02	0.53 ± 0.02				
PPgMA/Pglass 94/6 v/v	0.80 ± 0.03	0.20 ± 0.02	0.25 ± 0.03	0.40 ± 0.04	1.1x	3x	2x	1.5x
PPgMA/Pglass 90/10 v/v	0.75 ± 0.03	0.11 ± 0.02	0.15 ± 0.02	0.31 ± 0.07	1.2x	6x	4x	1.8x
PPgMA/Pglass 80/20 v/v	0.65 ± 0.03	0.009 ± 0.004	0.02 ± 0.004	0.09 ± 0.01	1.4x	75x	30x	6x

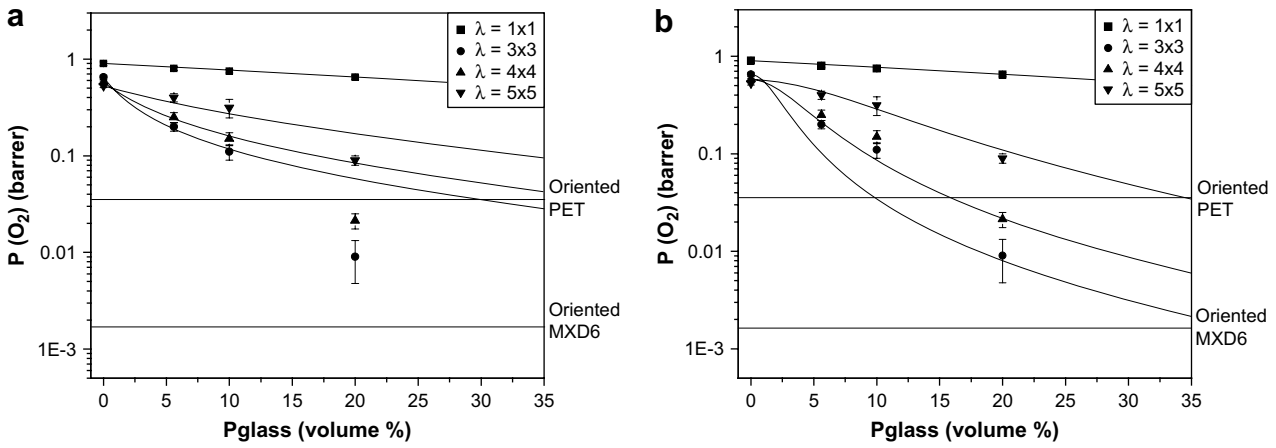

Fig. 5. Experimental data for oxygen permeability versus volume fraction of Pglass with various fits according to (a) Nielson equation (b) Cussler equation.

Specimens were cut from center region of the films for further characterization. The SEM images confirmed that biaxial stretching of the compression-molded films at a strain rate of 5% s^{-1} deformed the dispersed Pglass spheres into high aspect ratio platelets. The example in Fig. 4 shows the 90/10 v/v composite stretched to a target draw ratio of 4×4. Adhesion between the PPgMA matrix and the dispersed Pglass particles was good enough that stress transfer to the dispersed spheres transformed them into high aspect ratio platelets [18–22]. The platelet volume appeared to be considerably larger than the initial particle volume (Fig. 1) suggesting that the Pglass particles coalesced during stretching.

5. Oxygen permeability

Various models are used to describe the gas permeability of composite materials. It was anticipated that the permeability P of the compression-molded films would be described by the Maxwell model for randomly dispersed spherical particles [23].

$$\frac{P}{P_m} = 1 + \frac{3\phi_{Pglass}}{\left[\frac{(P_{Pglass}/P_m)+2}{(P_{Pglass}/P_m)-1}\right] - \phi_{Pglass}} \tag{2}$$

where P_{Pglass} and P_m are the permeabilities of the dispersed Pglass particles and the PPgMA matrix, respectively, and ϕ_{Pglass} is the volume fraction of Pglass. If the particles are platelet-shaped with aspect ratio α and oriented parallel to the polymer film surface, i.e., perpendicular to the permeation direction as in the biaxially stretched films, appropriate permeability models include those of Nielson [24]

$$\frac{P}{P_m} = \frac{1 - \phi_{Pglass}}{1 + \alpha\frac{\phi_{Pglass}}{2}} \tag{3}$$

or Cussler et al. [25]

$$\frac{P}{P_m} = \frac{1 - \phi_{Pglass}}{1 + \left(\alpha\frac{\phi_{Pglass}}{2}\right)^2} \tag{4}$$

Recently, Fredrickson and Bicerano [26,27] developed a rigorous solution for gas diffusion through a dispersion of impermeable disks that simplified to the Nielsen model in the dilute regime where the disk spacing exceeds the disk radius R, and to the Cussler model in the semidilute regime where the disk spacing is comparable to or smaller than R, but ϕ_{Pglass} remains much smaller than unity.

The oxygen permeability data are summarized in Table 3. The decrease in P of PPgMA with increasing area draw ratio was consistent with previous reports for biaxially stretched isotactic PP [28]. The presence of spherical Pglass particles in the unstretched composite decreased the permeability somewhat. The dependence of P on Pglass content was satisfactorily described by Eq. (2). Transformation of the spherical Pglass particles into platelets by biaxial stretching to a target draw ratio of 3×3 remarkably decreased the permeability. However, stretching to a higher target draw ratio resulted in some increase in the permeability, possibly due to breakup of the Pglass platelets and a reduction in the aspect ratio.

The permeability data for the stretched films were fit to the Nielsen model using the aspect ratio α as the only fitting parameter. Eq. (3) satisfactorily described the results for the lower Pglass loadings (96/6 and 90/10 v/v) with particle aspect ratios α of 80, 45, and 15 for target draw ratios of 3×3, 4×4 and 5×5, respectively, Fig. 5a. On the other hand, P of the composite with the highest Pglass content (80/20 v/v) was considerably lower than the prediction from Eq. (3) for all draw ratios. When the results for these films were compared against the prediction from Eq. (4) using the aspect ratios extracted from the Nielsen analysis, good agreement was obtained, Fig. 5b. It would seem that composites with 10 volume% Pglass or less fell in the dilute regime whereas 20 volume% Pglass was high enough to put the composite in the semidilute regime. The aspect ratios obtained by fitting the data were consistent with the platelet dimensions observed in the SEM images.

It is possible to calculate a platelet draw ratio using volume conservation and assuming that the spherical domains deform affinely into circular disks. From volume conservation

Table 4
Density values of biaxially oriented films drawn to various targeted draw ratios.

	Quenched	Annealed	3×3	4×4	5×5
PPgMA	0.9025 ± 0.0005	0.9145 ± 0.0005	0.9137 ± 0.0005	0.9130 ± 0.0005	0.9115 ± 0.0005
PPgMA/Pglass 94/6 v/v	1.070 ± 0.001	1.079 ± 0.001	1.071 ± 0.001	1.068 ± 0.005	1.055 ± 0.007
PPgMA/Pglass 90/10 v/v	1.162 ± 0.001	1.174 ± 0.001	1.168 ± 0.001	1.165 ± 0.005	1.158 ± 0.007
PPgMA/Pglass 80/20 v/v	1.431 ± 0.001	1.445 ± 0.001	1.424 ± 0.001	1.39 ± 0.01	1.32 ± 0.02

Table 5
Density values of PPgMA in biaxially oriented composite films drawn to various targeted draw ratios.

	Quenched	Annealed	3 × 3	4 × 4	5 × 5
PPgMA	0.9025	0.9145	0.9137	0.9130	0.9115
PPgMA/Pglass 94/6 v/v	0.9053	0.9148	0.9063	0.9031	0.8893
PPgMA/Pglass 90/10 v/v	0.8917	0.9050	0.8983	0.8950	0.8872
PPgMA/Pglass 80/20 v/v	0.8969	0.9142	0.8882	0.8460	0.7591

$$\frac{4}{3}\pi r^3 = \pi(\lambda r)^2 W \tag{5}$$

then

$$\alpha = \frac{L}{W} = \frac{2\lambda r}{W} = \frac{3}{2}\lambda^3 \tag{6}$$

where r is the radius of the spherical domains, λ is the balanced biaxial draw ratio, and L and W are the length and thickness of the circular disk, respectively. The aspect ratios calculated from Eq. (6) using the measured draw ratios in Table 3 were substantially higher than the effective values obtained from the permeability results for all the composites.

It was readily apparent that biaxial stretching transformed spherical Pglass particles into impermeable platelets that imparted dramatically reduced oxygen permeability. However, the model calculations suggested that even greater reductions were possible. Non-affine deformation of the Pglass particles due to viscosity differences or poor adhesion, or breakup into lower aspect ratio platelets, could have compromised the results. Alternatively, void formation during stretching might have had a role. This possibility was tested with density measurements, Table 4. In this case, the stretched samples were compared with an unstretched control that was annealed at the stretch temperature for 60 s. The decrease in density of PPgMA with increasing draw ratio was observed previously with biaxially stretched isotactic PP and was attributed to reduced crystallinity [28]. It should be recalled that the films were partially melted during the preheat period and they remained partially melted during the stretching process. Recrystallization during cooling was inhibited by orientation of the amorphous tie chains.

The density of the Pglass composites also decreased systematically with draw ratio. The decrease in density in the biaxially oriented composite films was more pronounced than in neat PPgMA suggesting that the Pglass platelets restricted the crystallization of the polymer matrix quite significantly. The density of the PPgMA in the biaxially oriented composites can be calculated according to Ref. [29]

$$\rho_{\mathrm{PPgMA}} = \frac{\rho_c - \phi_{\mathrm{Pglass}}\rho_{\mathrm{Pglass}}}{1 - \phi_{\mathrm{Pglass}}}$$

where ρ_c is the density of the composite, ϕ_{Pglass} is the volume fraction of Pglass and ρ_{Pglass} is the density of the Pglass. The results are given in Table 5. For the 94/6 and 90/10 v/v composites, the calculated density of the PPgMA phase decreased systematically with increasing glass content and with increasing draw ratio, but in all cases was substantially higher than the amorphous phase density of PP ($\rho_a = 0.853$ g cm^{-3} [28]). This was consistent with the hypothesis that the glass phase constrained crystallization of the PPgMA. Although cavitation may have been insignificant in the 94/6 and 90/10 films, it appeared to be substantial in the stretched 80/20 films. In the 80/20 v/v composite films biaxially oriented to targeted draw ratios of 4 × 4 and 5 × 5, the calculated density of the PPgMA phase was much lower than for the other composite films and indeed was less than the amorphous phase density of PP. At least in these cases, it appeared that cavitation had occurred and was at least one reason that full realization of the gas barrier potential of these composites was not realized. The thickness of the films restricted our ability to carry out DSC and verify any changes in percent crystallinity.

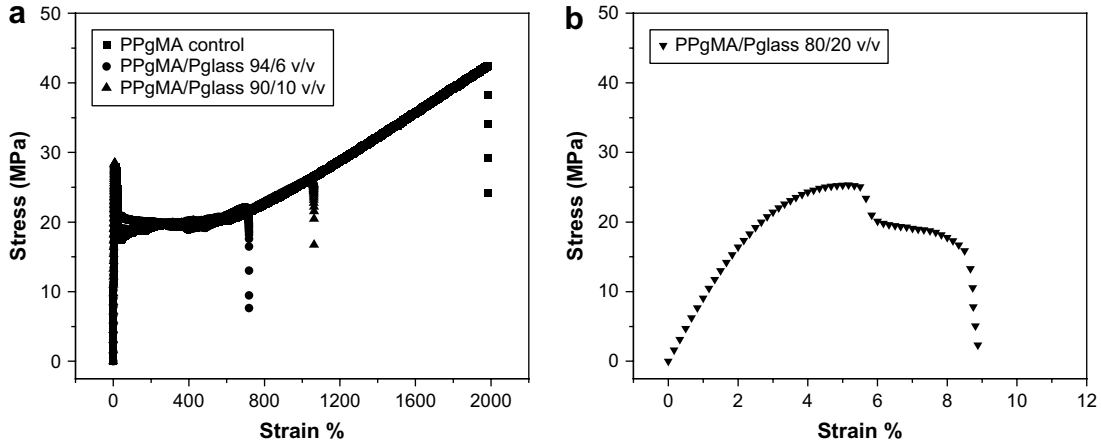

Fig. 6. Typical stress–strain curves for neat PPgMA and PPgMA/Pglass composites.

Table 6
Summary of tensile properties of unoriented neat PPgMA and PPgMA/Pglass composites.

	Modulus (GPa)	Yield stress (MPa)	Fracture stress (MPa)[a]	Elongation at break (%)
PPgMA	0.61 ± 0.01	27.6 ± 0.4	43.0 ± 1.0	2000 ± 100
PPgMA/Pglass 94/6 v/v	0.69 ± 0.03	28.4 ± 0.4	23.0 ± 1.0	750 ± 50
PPgMA/Pglass 90/10 v/v	0.72 ± 0.03	26.0 ± 1.0	26.0 ± 3.0	900 ± 150
PPgMA/Pglass 80/20 v/v	0.88 ± 0.05	24.8 ± 2.0	23.0 ± 3.0	10 ± 5

[a] Normalized to PPgMA volume%.

Table 7
Summary of tensile properties of biaxially oriented neat PPgMA and PPgMA/Pglass composites.

	Modulus (GPa)	Elongation at break (%)
PPgMA	1.15 ± 0.03	80 ± 20
PPgMA/Pglass 94/6 v/v	1.35 ± 0.10	50 ± 10
PPgMA/Pglass 90/10 v/v	1.46 ± 0.08	60 ± 10
PPgMA/Pglass 80/20 v/v	2.50 ± 0.20	50 ± 5

6. Mechanical properties

Fig. 6 shows the typical stress–strain behavior for the compression molded PPgMA/Pglass composites studied. Composites with up to 10 volume% Pglass showed ductile behavior with formation of a stable neck. Deformation occurred by uniform extension of the entire gauge section. A drop in the elongation at break and fracture stress was observed with the incorporation of up to 10 volume% Pglass in the composites as compared to the neat PPgMA. The stress–strain behavior of composites with 20 volume% Pglass began to resemble that of brittle solids with significant drop in elongation at break. Debonding occurs at yielding between the glass particles and polymer matrix. Increasing the Pglass concentration to 20 volume% lead to formation of narrow craze-like deformation zones causing it to fail in a quasi brittle manner [30]. The modulus of the composite materials increased almost linearly with the addition of Pglass and took values up to 50% higher than that of neat PPgMA, Table 6.

The stress–strain behavior of the biaxially oriented PPgMA/Pglass composite films was also studied. Table 7 gives the modulus and elongation at break values for the biaxially oriented composite films drawn to 3×3. The modulus of the neat PPgMA increased from 0.65 GPa to 1.1 GPa. The significant improvement in the modulus was attributed to the orientation of the polymer chains during the biaxial orientation process. The modulus of the composite films also increased by a factor of 1.3–2.2x depending on the volume% of the Pglass in the composite.

7. Conclusions

The oxygen barrier of PPgMA was significantly improved by incorporating Pglass as impermeable inclusions. The Pglass, which was dispersed as spherical droplets in the compression-molded films, elongated into high aspect ratio platelets during the stretching process. The largest reduction in oxygen permeability was obtained by stretching a composite with 20 volume% Pglass to a target draw ratio of 3×3. For all the composites, the largest reduction in permeability was obtained by stretching to a target draw ratio of 3×3. Stretching the composites to higher draw ratios resulted in some increase in permeability which was attributed to breakup of the platelet-shaped particles and possibly to some cavitation that occurred during stretching. The reduced permeability of the biaxially oriented films was described using either the Nielson or Cussler models depending on the volume of the Pglass in the composite. The particle aspect ratio obtained by fitting the experimental data to the various models ranged from 80 for a target draw ratio of 3×3 to 15 for a target draw ratio of 5×5. These results were within the range observed by SEM experiments. The glass platelets imparted a higher modulus to the stretched films while reducing the elongation at break only slightly.

Acknowledgement

This material is based upon work supported by the National Science Foundation under Grant No. DMR 0423914.

References

[1] Bissot TC. In: Koros WJ, editor. Barrier polymers and structures. Washington, DC: American Chemical Society; 1990. p. 225–38.
[2] Sekelik DJ, Stepanov EV, Nazarenko S, Schiraldi DA, Hiltner A, Baer E. J Polym Sci Part B Polym Phys 1999;37:847–57.
[3] Tick PA. US 4379070; 1983.
[4] Tick PA. Phys Chem Glasses 1984;25:149–54.
[5] Shaw CM, Shelby JE. Phys Chem Glasses 1988;29:49–53.
[6] Shaw CM, Shelby JE. Phys Chem Glasses 1988;29:87–90.
[7] Xu XJ, Day DE. Phys Chem Glasses 1990;31:183–7.
[8] Frayer PD. US 6103810; 2000.
[9] Adalja SB, Otaigbe JU, Thalacker J. Polym Eng Sci 2001;41:1055–67.
[10] Urman K, Otaigbe JU. Prog Polym Sci 2007;32:1462–98.
[11] Jang J, Lee DK. Polymer 2004;45:1599.
[12] Utracki LA, Shi ZH. Polym Eng Sci 1992;32:1824–33.
[13] Wu S. Polymer 1985;26:1855–63.
[14] Li T, Topolkaraev VA, Hiltner A, Baer E, Ji XZ, Quirk RP. J Polym Sci Part B Polym Phys 1995;33:667–83.
[15] Li T, Carfagna C, Topolkaraev VA, Hiltner A, Baer E, Ji XZ, et al. Adv Chem Series 1996;252:335–50.
[16] Majumdar B, Keshkula H, Paul DR. Polymer 1994;35:1386–98.
[17] Dias P, Lin YJ, Hiltner A, Baer E, Chen HY, Chum SP. J Appl Polym Sci 2008;107:1730–6.
[18] Favis BD. In: Paul DR, Bucknall CB, editors. Polymer blends. New York: Wiley; 2000. p. 501–37.
[19] Gonzalez-Nunez R, De Kee D, Favis BD. Polymer 1996;37:4689–93.
[20] Lee SY, Kim SC. Polym Eng Sci 1997;37:463–75.
[21] Young RT, McLeod MA, Baird DG. Polym Composites 2000;21:900–17.
[22] Urman K, Schweizer T, Otaigbe JU. Rheol Acta 2007;46:989–1001.
[23] Barrer RM. In: Crank J, Park GS, editors. Diffusion in polymers. New York: Academic; 1968. p. 165–217.
[24] Nielson LE. J Macromol Chem 1967;A1(5):929–42.
[25] Cussler EL, Stephanie EH, William JW, Rutherford A. J Membr Sci 1988;38:161–74.
[26] Fredrickson GH, Bicerno J. J Chem Phys 1999;110:2181–8.
[27] Nazarenko S, Meneghetti P, Julmon P, Olson BG, Qutubuddin S. J Polym Sci Part B Polym Phys 2007;45:1733–53.
[28] Lin YJ, Dias P, Chen HY, Hiltner A, Baer E. Polymer 2008;49:2578–86.
[29] Yee RY, Stephens TS. Thermochim Acta 1996;272:191–9.
[30] Dubnikova IL, Muravin DK, Oshmyan VG. Polym Eng Sci 1997;37:1301–13.